Article

Not peer-reviewed version

New Sesterterpenes from the Antarctic Sponge Suberites sp.

Stine S.H. Olsen , Sydney K Morrow , Julia L Szabo , Michael N. Teng , Kim C. Tran , Charles D. Amsler , James B. McClintock , Bill. J. Baker *

Posted Date: 6 November 2024

doi: 10.20944/preprints202411.0376.v1

Keywords: Suberites sp.; sesterterpenes; suberitane; porifera; Antarctica; RSV

Article

New Sesterterpenes from the Antarctic Sponge *Suberites* sp.

Stine S. H. Olsen [1], Sydney K. Morrow [1], Julia L. Szabo [1], Michael N. Teng [2], Kim C. Tran [2], Charles D. Amsler [3], James B. McClintock [3] and Bill. J. Baker [1,*]

[1] Department of Chemistry, University of South Florida, 4202 E. Fowler Avenue, CHE205, Tampa, Florida, 33620, USA
[2] Department of Internal Medicine, University of South Florida, Tampa, FL, 33612, USA
[3] Department of Biology, University of Alabama at Birmingham, 1300 University Blvd, Birmingham, AL 35233, USA
* Correspondence: bjbaker@usf.edu; Tel.: +1-(813)-974-1967

Abstract: Chemical investigation of the Antarctic sponge *Suberites* sp. has previously led to the identification of new suberitane derivatives, some of which show bioactivity toward the respiratory syncytial virus (RSV). Our ongoing NMR-guided investigation of new specimens of the sponge resulted in the isolation of five new analogs (**1-5**), the previously reported suberitenones A-D (**6-9**) and oxaspirosuberitenone (**10**). Suberitenone K (**1**) was characterized as the 8-keto derivative of suberitenone A, while three new phenols, suberitandiol (**2**), abeosuberitandiol (**3**), and furanosuberitandiol (**4**), and the degraded sesterterpene norsuberitenone B (**5**) were also found. **3** displays a ring contraction while **4** has a new dihydrofuran ring. Structural characterization was achieved by a combination of NMR, HR-MS, and X-ray diffraction. Suberitenone D and the new metabolite suberitenone K showed moderate activity towards RSV, while norsuberitenone B and furanosuberitandiol were found to have mild activity.

Keywords: *Suberites* sp.; sesterterpenes; suberitane; porifera; Antarctica; RSV

1. Introduction

With an expansive range and biogeographic isolation, the waters of the Southern Ocean surrounding Antarctica host rich and diverse marine benthic invertebrate communities [1,2]. Marine sponges often act as the dominant taxa in many benthic habitats in the region, and these organisms often produce chemical defences to survive in communities structured by biotic influences like predation and competition for limited resources [2]. Sponges from Antarctica have been found to produce a wide variety of chemical compounds, including terpenes [3]. Naturally occurring terpenes have interesting chemical structures that exhibit bioactivities such as antimicrobial, anticancer, and anti-inflammatory properties that may have pharmaceutical applications in the field of drug discovery [4–6]. The isolation of these compounds reveals auspicious results for bioprospecting efforts in Antarctica [4].

Suberites is a genus of the family Suberitidae. These organisms can be found across various oceanic habitats including coral reefs, rocky intertidal zones, and deep sea environments [2]. *Suberites* spp. play an important role in the ecosystems they inhabit through their water filtration and benthic shaping qualities [2]. The genus *Suberites* belongs to the largest and most diverse class of sponges, Demospongiae, which leaves room for vast research to be conducted on the natural product compounds they possess. Our research group has previously studied Antarctic *Suberites* sp. and discovered a variety of unreported sesterterpenes, including neosuberitenone, which was characterized by a new carbon scaffold, as well as six suberitenone derivatives, an ansellane-type terpenoid, and a highly degraded sesterterpene [7]. Some of these compounds were reported with antiviral activity [7].

 doi:10.20944/preprints202411.0376.v1

Herein, we report on our continuing investigation of the Antarctic sponge *Suberites* sp.. New specimens of the sponge were subject to ^{1}H NMR-guided purification using reverse-phase high-performance liquid chromatography (HPLC), resulting in the isolation of five new suberitane derivatives, three being derivatives of suberiphenol [8]. Additional supplies of our previously published suberitenones were isolated together with the two major metabolites suberitenone A (**6**) and B (**7**), and the minor metabolites suberitenone C (**8**), D (**9**), and oxaspirosuberitenone (**10**) [7–10]. We report the structure elucidation of the previously unreported compounds and their RSV antiviral activity.

2. Results and Discussion

The molecular formula of suberitenone K (**1**) was determined to be $C_{27}H_{38}O_5$ based on HRESIMS data ($[M + Na]^+$ *m*/*z* 465.2622) and corroborated by the ^{1}H and ^{13}C NMR spectra (Table 1). The ^{13}C NMR spectrum indicated **1** to have four olefinic carbons, including two methines and two olefinic quaternary signals, as well as three carbonyls. These account for five degrees of unsaturation, indicating **1** to have a four ring system. The remaining 20 carbons are accounted for by three quaternary carbons, three aliphatic methines, two oxygen-bearing methines, six methyl groups, and six methylene groups. The ^{1}H NMR data (Table 1) showed two oxygen-bearing methines at δ_H 4.25 (H-1) and δ_H 5.56 (H-13), two olefinic methines at δ_H 6.80 (H-2) and δ_H 6.40 (H-22), three aliphatic methines at δ_H 3.35 (H-6), δ_H 1.96 (H-10), and δ_H 1.23 (H-14), and six singlet methyl groups. These NMR data indicated this compound to be structurally related to other reported compounds from *Suberites* sp. (Figure 1), known as the suberitane carbon skeleton [9].

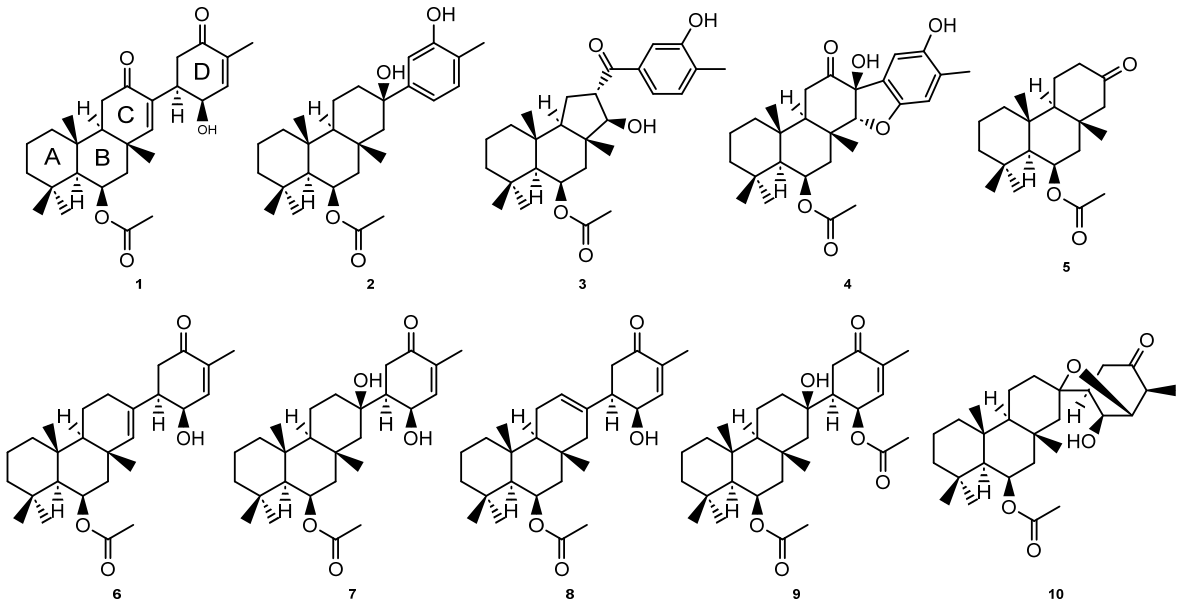

Figure 1. Sesterterpenes isolated from the Antarctic sponge *Suberites* sp.

The ring A partial structure could be established by a combination of COSY and HMBC correlations (Figure 2). Geminal methyl groups H_3-20 and H_3-25 (δ_H 0.94, 1.06) anchor the spin system, both displaying HMBC correlations to C-14, C-18, and C-19 (δ_C 57.3, 45.3, and 35.1, respectively). The methine H-14 (δ_H 1.23) displayed HMBC correlations to methyl groups C-20 (δ_C 33.3) and C-24 (δ_C 17.4) and the quaternary carbons C-15 (δ_C 38.2) and C-19. H_3-24 (δ_H 1.34) had HMBC correlations to C-10 (δ_C 54.9), C-14, C-15, and methylene C-16 (δ_C 42.2). The COSY data further connects H_2-17 (δ_H 1.81/1.51) to H_2-16 (δ_H 1.69/0.98) and H_2-18 (δ_H 1.41/1.26), resulting in ring A.

 doi:10.20944/preprints202411.0376.v1

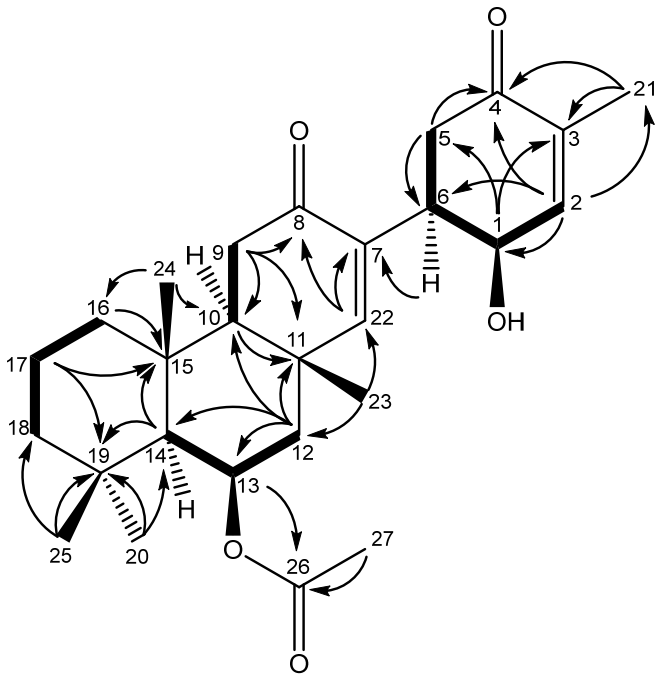

Figure 2. Key COSY (bold) and HMBC (arrow) correlations of suberitenone K (**1**).

Extending the spin system, COSY correlations were observed between H-14 and oxymethine H-13 (δ_H 5.59), which further correlated with H_2-12a/12b (δ_H 2.06/1.66). H_2-12 had HMBC correlations to C-10, C-11 (δ_C 37.7), C-13 (δ_C 72.0), and C-14, closing the six-membered ring B with quaternary carbon C-15 between C-10 and C-14 based on the previously described HMBC correlation between H_3-24 and C-10. The singlet methyl H_3-23 (δ_H 1.29) had HMBC correlations to C-10, C-11, C-12, and the olefinic methine C-22 (δ_C 160.7), placing the methyl on quaternary carbon C-11. H_2-9 (δ_H 2.52/2.50) showed HMBC correlations to carbonyl C-8 (δ_C 202.1), C-10, and C-11. HMBC correlations from H-22 to C-8 and the olefinic quaternary carbon C-7 (δ_C 134.2) connects carbonyl C-8 and olefinic methine C-22 with C-7, completing ring C.

A separate spin system comprising ring D was constructed based on COSY correlations from oxymethine H-1 (δ_H 4.25) to aliphatic methine H-6 (δ_H 3.35) and olefinic methine H-2 (δ_H 6.80). Further, H-2 showed HMBC correlations to C-1 (δ_C 65.2), C-4 (δ_C 202.2), C-6 (δ_C 38.5), and C-21 (δ_C 15.7). The singlet methyl group H_3-21 (δ_H 15.7) displayed HMBC correlations to C-2 (δ_C 145.3), C-3 (δ_C 137.2), and C-4, placing it on the quaternary carbon C-3 with the olefinic methine (C-2) and ketone (C-4) on each side. The non-equivalent methylene H_2-5a/5b (δ_H 2.75/2.15) had HMBC correlations with C-1, C-4, and C-6, closing ring D. This was supported by COSY correlations from methine H-6 to H-1 and H_2-5a/5b.

The two spin systems were joined based on HMBC correlation between H-5a and H-6 with olefinic quaternary carbon C-7 (δ_C 134.2), establishing the suberitane backbone. The acetoxy group can be placed on oxygen-bearing C-13 based on the deshielded shift of both its carbon (δ_C 72.0) and proton (δ_H 5.59) and HMBC correlations from H-13 to C-26 (δ_C 172.1), completing the planar structure of suberitenone K (**1**).

The relative stereochemistry was determined by key NOE correlations between H_3-20, H-13, and H-14 and further between H-14 and H-10. H_3-23 has an NOE correlation to the acetoxy methyl, placing those on the same face of the ring. H_3-25 has an NOE correlation to H_3-24 placing those on the same face as the acetoxy, as H_3-25 is opposite to H_3-20. The relationship of H-1 and H-6 were determined to be *syn* to each other based on their coupling constants of J= 4.0. NOE correlations and coupling constants were used to determine **1** to share stereocenters of the same orientation as the known compound suberitenone A (**6**), suggesting they have the same absolute configuration of 1*R*,6*R*,10*S*,11*S*,13*R*,14*S*,15*R* as previously determined by Shin et al. [9] for suberitenone A using a

 doi:10.20944/preprints202411.0376.v1

modified Mosher's method and CD analysis as well as our analysis of suberitenone E, which was confirmed by X-ray diffraction [7].

Table 1. NMR Data for Suberitenone K (**1**) (600 (^{1}H) and 150 (^{13}C) MHz, MeOD).

Position	δ_C, type	δ_H (mult., (*J*))	gCOSY	gHMBC
1	65.2, CH	4.25, dd (4.5, 5.0)	2, 6	2, 3, 5
2	145.3, CH	6.80, dq (1.3, 5.6)	1, 21	1, 4, 6, 21
3	137.2, C			
4	202.2*, C			
5a	37.6, C	2.75, dd (13.5, 16.1)	5b, 6	1, 4, 6, 7
5b		2.15, dd (3.5, 16.1)	5a, 6	1, 3, 4, 6, 7
6	38.5, CH	3.35, o/l*	1, 5a, 5b	1, 5, 7, 22
7	134.2, C			
8	202.1*, C			
9a	35.6, CH_2	2.52, d (12.6)	9b, 10	8, 10, 11
9b		2.50, d (4.9)	9a, 10	
10	54.9, CH	1.96, dd (5.4, 12.5)	9a, 9b	8, 9, 11, 22, 23, 24
11	37.7, C			
12a	43.9, CH_2	2.06, o/l*	12b, 13	10, 11, 13, 14, 22, 23
12b		1.66, o/l*	12a, 13	11, 22, 23
13	72.0, CH	5.59, ddd (2.6, 2.8, 2.9)	12a, 12b, 14	12, 14, 26
14	57.3, CH	1.23, o/l*	13	15, 19, 20, 24
15	38.2, C			
16a	42.2, CH_2	1.69, o/l*	16b, 17a, 17b	15
16b		0.98, o/l*	16a, 17a, 17b	
17a	19.5, CH_2	1.81, o/l*	16a, 16b, 17b, 18a, 18b	
17b		1.51, qd (3.1, 14.3)	16a, 16b, 17a, 18a, 18b	15, 19
18a	45.3, CH_2	1.41, ddd (3.5, 4.0, 12.9)	17a, 17b, 18b	16
18b		1.26, o/l*	17a, 17b, 18a	
19	35.1, C			
20	33.3, CH_3	0.94, s		14, 18, 19, 25
21	15.7, CH_3	1.79, s		2, 3, 4
22	160.7, C	6.40, s		6, 7, 8, 10, 12, 23
23	20.9, CH_3	1.29, s		10, 11, 12, 22
24	17.4, CH_3	1.34, s		10, 14, 15, 16
25	23.7, CH_3	1.06, s		14, 18, 19, 20
26	172.1, C			
27	21.9, CH_3	2.07, s		26

* Overlapping 1H and 13C NMR signals, 2D assignments based on proximity likelihood.

Suberitandiol (**2**) was determined to have the molecular formula $C_{27}H_{40}O_4$ by the negative ion formate adduct ($[M + CHOO]^-$ 473.2908 *m/z*). The NMR data of **2** (Table 2) suggest ring A and B to be as found in **1**. Similarly to **1**, **2** has six methyl groups, one being part of the acetoxy group on C-13 (δ_C 70.6). The H_3-23 (δ_H 1.43) methyl has HMBC correlations to C-10 (δ_C 58.9), C-11 (δ_C 34.8), C-12 (δ_C 46.7), and C-22 (δ_C 57.2), being placed on the quaternary carbon C-11, connecting ring B and C as shown for **1**. C-22 for **1** was an olefinic methine, but for **2** was found as a non-equivalent methylene. Ring C was further verified and connected through H-22a (δ_H 1.57) with HMBC correlations to C-8 (δ_C 41.1), C-10, C-11, C-23 (δ_C 22.7), and quaternary carbon C-7 (δ_C 74.4) as shown in Figure 3. Methylene H-9a (δ_H 1.86) displays COSY correlations to H_2-8 (δ_H 1.90) and H-10 (δ_H 1.06), establishing much of ring C. Ring C was completed between C-8 and C-9 by H-9b (δ_H 1.69), which demonstrated HMBC correlations to C-7, C-10, and C-11. With ring D left, three olefinic/aromatic methines, one deshielded methyl group, three quaternary carbons and two oxygens remain left to account. The

 doi:10.20944/preprints202411.0376.v1

three olefinic/aromatic methines and three quaternary carbons make up an aromatic ring with three substituents. The methine H-2 (δ_H 7.07 (d)) had COSY correlations to methine H-1 (δ_H 6.90), creating an olefinic bond and suggesting the loss of the oxygen-bearing methine previously observed in **1**. Further, H-2 had HMBC correlations to the quaternary carbons C-4 (δ_C 152.6) and C-6 (δ_C 149.5) and the methyl C-21 (δ_C 15.3), as observed for **1.** The third methine (H-5, δ_H 6.95) is a singlet with HMBC correlations to C-1 (δ_C 116.6) and C-3 (δ_C 122.0). The H_3-21 methyl (δ_H 2.23) had HMBC correlations to C-2 (δ_C 130.7), C-3 (δ_C 122.0), and C-4, placing the methyl on the quaternary carbon C-3. The aromatic methines H-1 and H-5 both have HMBC correlations to C-7, suggesting a bridge between C-6 and C-7, connecting ring C and D. This leaves an open valence on C-4 and C-7, with two oxygens and two protons left to account for, indicating an hydroxyl group on each to complete the planar structure of **2**. These assignments are supported by their deshielded shifts. The 3D structure was solved by comparing NOE and coupling constants to **1**. The tertiary alcohol at C-7 was deduced by NOE correlations in DMSO-d_6 from OH-7 (δ_H 4.38) to H_3-23 (δ_H 1.34). The absolute configuration is proposed as 7*R*,10*S*,11*S*,13*R*,14*S*,15*R* based on similarly to the known compound suberitenone B [9].

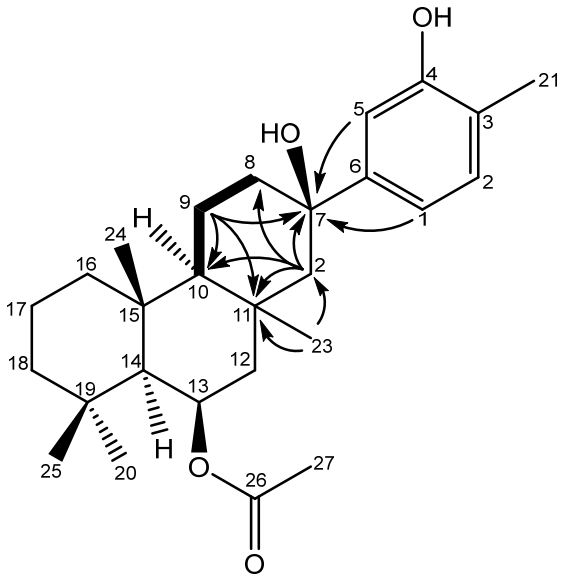

Figure 3. Key COSY (bold) and HMBC (arrows) correlations of suberitandiol (**2**), highlighting changes in ring C.

Abeosuberitandiol (**3**) was found to have the formula $C_{27}H_{38}O_5$ based on its ^1H and ^{13}C NMR data (Table 2) and the formate anion adduct at 487.2697 *m/z*. The three aromatic methines and its 2D data (Figure S27-29) indicate **3** to have the rings A, B, and D as found for **2**. Figure 4 highlights the HMBC and COSY correlations to establish the differences found in ring C. H_3-23 (δ_H 1.16) has HMBC correlations to C-10 (δ_C 56.4), C-12 (δ_C 42.6), and C-22 (δ_C 83.5) as shown for the other structures, however, differently from **1** and **2**, H-22 (δ_H 4.02) has the shift of an oxygen-bearing methine. H-22 has COSY correlation to methine H-7 (δ_H 3.58), which further shows COSY correlations to the non-equivalent methylene H_2-9a/9b (δ_H 2.09/1.66). H_2-9a/9b has COSY correlation to H-10 (δ_H 1.30), completing ring C as a five-membered ring. H-9a has HMBC correlations to C-7 (δ_C 50.1), C-10 (δ_C 56.4), and the carbonyl C-8 (δ_C 202.1). H-22 and H-1 (δ_H 7.43) display HMBC correlations to C-8, as shown in Figure 4, suggesting the ketone acts as a bridge between ring C and D. The absolute configuration was deduced as earlier, showing the relative orientation of chiral centers 10*R**,11*R**,13*R**,14*S**,15*R**. NOE correlations between H-7/H_3-23 and H-10/H-22 places H-7 and H-22 *anti* to one another, suggesting the absolute configuration of **3** to be 7*S*,10*R*,11*R*,13*R*,14*S*,15*R*,22*R*.

Preprints.org (www.preprints.org) | NOT PEER-REVIEWED | Posted: 6 November 2024 doi:10.20944/preprints202411.0376.v1

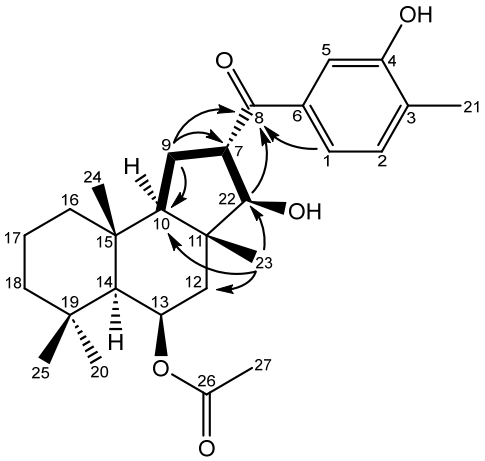

Figure 4. Key COSY (bold) and HMBC (arrow) correlations of abeosuberitandiol (**3**) , highlighting changes in ring.

Table 2. ^{1}H and ^{13}C NMR Data for **2-4** (400 (^{1}H) and 100 (^{13}C) MHz, $CDCl_3$).

Position	2		3		4	
	δ_C, type	δ_H (mult., (*J*))	δ_C, type	δ_H (mult., (*J*))	δ_C, type	δ_H (mult., (*J*))
1	116.6, CH	6.90, d (7.8)	121.4, CH	7.43, dd (1.0, 7.9)	155.3, C	
2	130.7, CH	7.07, d (7.9)	131.0, CH	7.19, d (7.8)	112.1, CH	6.70, s
3	122.0, C		130.6, C		128.4, C	
4	153.6, C		154.2, C		148.4, C	
5	111.4, CH	6.94, s	114.5, CH	7.41, d (1.0)	109.7, CH	6.42, s
6	149.5, C		136.0, C		124.2, C	
7	74.4, C		50.1, CH	3.58, ddd (4.0, 7.9, 11.9)	83.3, C	
8	41.1, CH_2	1.90, o/l*	202.1, C		210.8, C	
9a	17.5, CH_2	1.86, o/l*	26.2, CH_2	2.09, o/l*	33.9, CH_2	2.48, dd (10.6, 19.0)
9b		1.69, o/l*		1.66, ddd (3.0, 3.5, 12.8)		2.33, dd (19.1, 9.0)
10	58.9, CH	1.06, o/l*	56.4, CH	1.30, dd (7.1, 12.9)	45.9, CH	1.88, t (9.6)
11	34.8, C		43.1, C		38.3, C	
12a	46.7, CH_2	1.92, o/l*	42.6, CH_2	2.18, dd (2.1, 14.5)	38.9, CH_2	2.29, dd (4.2, 15.1)
12b		1.27, o/l*		1.39, o/l*		1.82, dd (2.4, 15.0)
13	70.6, CH	5.49, dt (2.5, 3.1)	70.7, CH	5.51, br dt (2.4, 2.5)	69.8, CH	5.64, td (2.1, 3.7)
14	56.8, CH	1.08, d (2.1)	57.5, CH	1.01, o/l*	55.2, CH	1.04, d (1.6)
15	37.2, C		36.9, C		37.4, C	
16a	41.9, CH_2	1.82, o/l*	41.5, CH_2	1.40, o/l*	41.8, CH_2	1.37, o/l*
16b		0.92, o/l*		0.94, o/l*		0.76, dt (2.8, 12.2)
17a	18.6, CH_2	1.75, o/l*	18.1, CH_2	1.70, o/l*	18.1, CH_2	1.62, m
17b		1.50, o/l*		1.41, o/l*		1.37, o/l*
18a	44.3, CH_2	1.39, o/l*	44.3, CH_2	1.39, o/l*	43.6, CH_2	1.36, o/l*
18b		1.20, o/l*		1.20, o/l*		1.17, dd (2.5, 13.7)
19	34.1, C		33.7, C		33.8, C	
20	32.9, CH_3	0.94, s	33.0, CH_3	0.92, s	33.1, CH_3	0.98, s
21	15.3, CH_3	2.23, s	16.1, CH_3	2.30, s	16.6, CH_3	2.23, s
22a	57.2, CH_2	1.59, d (14.3)	83.5, CH	4.02, d (7.8)	97.4, CH	4.19, s
22b		1.51, o/l*				
23	22.7, CH_3	1.43, s	14.2, CH_3	1.16, s	18.9, CH_3	1.00, s

 doi:10.20944/preprints202411.0376.v1

24	17.3, CH_3	1.25, s	16.7, CH_3	1.26, s	16.3, CH_3	1.26, s
25	23.0, CH_3	1.03, s	22.9, CH_3	1.02, s	23.2, CH_3	1.00, s
26	170.6, C		170.4, C		170.2, C	
27	21.9, CH_3	2.07, s	21.8, CH_3	2.08, s	21.8, CH_3	2.06, s

* Overlapping 1H NMR signals, 2D assignments based on proximity likelihood.

Furanosuberitandiol (**4**) was found with the molecular formula $C_{27}H_{36}O_6$, determined by the ^{1}H and ^{13}C NMR data (Table 2) and the (-)HRESIMS ($[M + CHOO]^-$ 501.2489 *m*/*z*). The formula suggests the structure to have ten degrees of unsaturation. The NMR data indicate **4** to have an aromatic ring, as observed for **2** and **3**, and two carbonyl groups. This leaves **4** with 5 rings. Figure 5 highlights the key HMBC and COSY correlations to establish the aromatic ring, and further differences in ring C. Its NMR data (Table S4) suggests **4** to have the same A/B ring system observed for **1**. Ring D differs in having two aromatic methines: C-2 (δ_C 112.1) and C-5 (δ_C 109.7). For **2** and **3**, C-1 was observed as a methine; however, it is found in **4** as a quaternary carbon with a deshielded shift (δ_C 155.3), suggesting oxygen substitution. H_3-23 (δ_H 1.00) had HMBC correlations to C-10 (δ_C 45.9) and C-22 (δ_C 97.4), suggesting C-22 to be oxygen-bearing, as shown in **3**. H-22 (δ_H 4.19) displays HMBC correlations to C-1 (δ_C 155.3), C-7 (δ_C 83.3), C-8 (δ_C 210.8), C-10 (δ_C 45.9), C-11 (δ_C 38.3), and C-23 (δ_C 18.9), suggesting a bridge between C-1 and C-22 through an oxygen. The non-equivalent methylene H-9a (δ_H 2.48) had COSY correlation to H-10 (δ_H 1.88) and HMBC correlations to quaternary carbon C-7 (δ_C 83.3) and carbonyl C-8 (δ_C 210.8), establishing further connectivity of ring C. The H-9a and H-22 correlations to C-7 and C-8 suggests completion of ring C between C-7 and C-22. To complete the planar structure, a hydroxyl group is left to account for and one and two valences are open on C-6 and C-7, respectively. This suggests the hydroxy group to be placed on the oxygen-bearing C-7 and a bridge between C-6 and C-7, establishing the fifth ring system. NOE correlations and coupling constants as described earlier were used to propose the absolute configuration of **5**. Key correlations between H_3-23 and H-22 determined a *syn* relationship for these protons, while the C-7 tertiary alcohol was placed on the same face as H-22 and H_3-23, as shown for **3** and suberitenone B [9]. This was corroborated by key NOE correlations in $(CD_3)_2SO$ between OH-7/H-22 and a weak correlation between OH-7/H_3-23 (Figure S42), giving **5** the proposed absolute configuration of 7*S*,10*R*,11*R*,13*R*,14*S*,15*R*,22*R*.

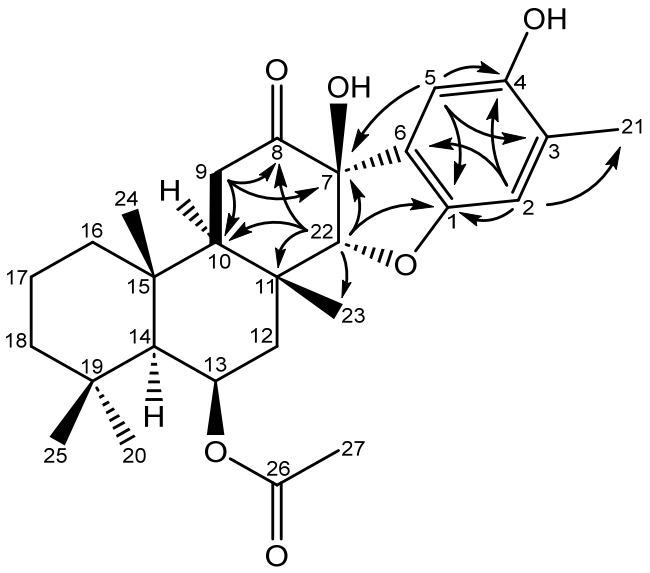

Figure 5. Key COSY (bold) and HMBC (arrow) correlations of furanosuberitandiol (**4**), highlighting changes in ring C and D.

Norsuberitenone B (**5**) was isolated as a white crystal with the molecular formula $C_{20}H_{32}O_3$ based on the *m*/*z* 321.2433 proton adduct of the (+)HRESIMS. Its formula indicates five degrees of unsaturation with two being carbonyl groups, suggesting a three-ring system. Its NMR data (Table

 doi:10.20944/preprints202411.0376.v1

S5) suggests **5** to have a similar ring system as shown for **1**, but lacking ring D. HMBC correlations from the methyl groups H_3-15 (δ_H 0.97) and H_3-18 (δ_H 1.02) to C-9 (δ_C 56.5), C-13 (δ_C 44.0), and C-14 (δ_C 34.0) and from H_3-17 (δ_H 1.23) to C-5 (δ_C 56.6), C-10 (δ_C 37.7), and C-11 (δ_C 42.3) suggests **5** to have a similar ring system for ring A and B as shown for previous suberitane compounds. The H_3-20 (δ_H 2.05) and its HMBC correlation to carbonyl C-19 (δ_C 170.3) suggests the presence of the acetoxy group on oxygen-bearing C-8 (δ_H 70.0). H_3-16 (δ_H 1.06) had HMBC correlations to C-1 (δ_C 59.6), C-5, C-6 (δ_C 37.9), and C-7 (δ_C 45.7), suggesting its place on the quaternary carbon C-6. The methylene H-1b (δ_H 2.03) and H-3b (δ_H 2.29) have HMBC correlations to a ketone (C-2: δ_C 210.9), suggesting a ketone to have replaced the tertiary alcohol bridging to ring D in **2**. The stereochemistry was determined by key NOE correlations from H_3-15 to H-8 (δ_H 5.52) and H-9 (δ_H 1.15) and further between H-9 and H-5 (δ_H 1.50). NOE correlations were observed between H_3-16 and the acetyl methyl group. X-ray diffraction (Figure 6) confirmed the structure and determined the absolute configuration to be 5*S*,6*S*,8*R*,9*S*,10*R*.

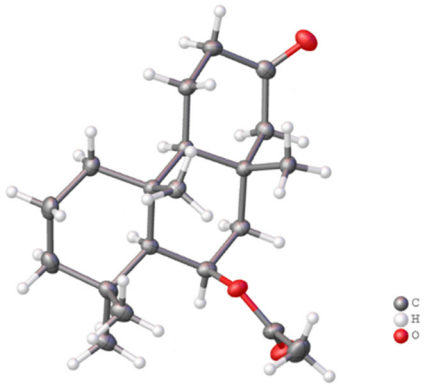

(**a**) (**b**)

Figure 2. (**a**) Key COSY (bold) and HMBC (arrow) correlations of **5**; (**b**) XRD of **5**.

Biosynthetically, the suberitane class differs from many other sesterterpenes due to the pendant ring D [9]. A proposed biosynthetic pathway of newly reported metabolites **1**-**5** is presented in Figure 7. The degraded suberitenone, norsuberitenone B (**5**), could be rationalized as the elimination product of ring D from suberitenone B. Compound **1** can be derived from the oxidation of a tetracyclic intermediate, as shown in Figure 7. The phenolic compounds **2**-**4** are perhaps derived from a protonation-catalyzed dehydration of the alcohol allylic to the α,β-unsaturated ketone.

 doi:10.20944/preprints202411.0376.v1

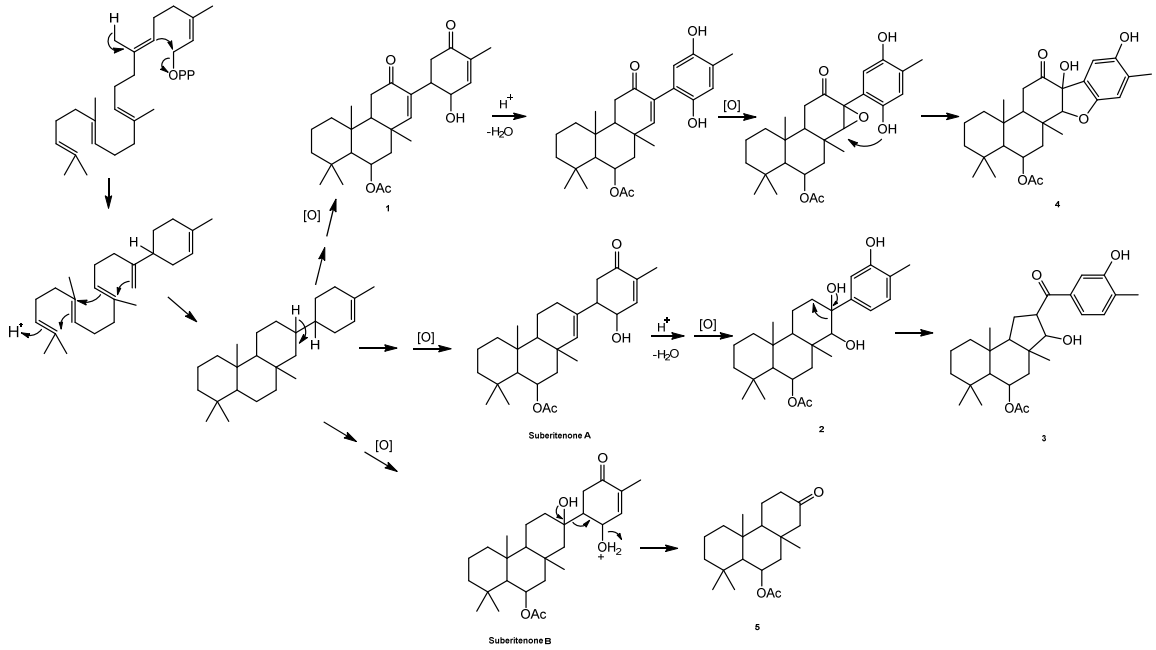

Figure 7. Proposed biogenesis of compounds **1**-**5**.

Bracegirdle et al. reported RSV activity for the known compounds suberitenone A (**6**) and B (**7**) with IC_{50} values of 7.8 μM and 3.2 μM, respectively, while the compounds suberitenone F, G, and H showed moderate activity [7]. Herein, we report weak RSV activity for suberitenone D (**9**) (Table 3), while the others displayed no activity. A decrease in activity is shown with the degraded sesterterpene **5** relative to suberitenone B, suggesting the presence of ring D to be important for further structure-activity relationship studies. Furthermore, no activity was shown for **2** and **3**, suggesting the importance of the α,β-unsaturated ketone on ring D. Suberitenone D has a decrease in activity compared to suberitenone B, with the only structural difference being the acetoxy replacing the hydroxyl group on ring D. Suberitenone C showed no activity and **1** displayed moderate activity, suggesting the $\Delta^{7(22)}$ olefin is favourable over the Δ^{8} olefin, but an α,β-unsaturated ketone on ring C will decrease the activity.

Table 3. RSV antiviral activity (IC_{50}).

Compound	IC_{50} (μM)
1	41.8
2	>50
3	>50
4	>50
5	>50
9	15.1

3. Materials and Methods

3.1. General Experimental Procedures

Optical rotations were measured using an AutoPol IV digital polarimeter at 589 nm with a 1 dm path length cell. UV/Vis spectra were extracted from HPLC chromatograms. NMR spectra were acquired using a Bruker Neo 400 MHz broadband spectrophotometer with a cryoprobe or a Bruker Neo 600 MHz broadband spectrophotometer. The residual solvent peaks were used as an internal chemical shift reference ($CDCl_3$: δ_C 77.0; δ_H 7.27, MeOD: δ_C 49.0; δ_H 3.31, $(CD_3)_2SO$: δ_C 39.5; δ_H 2.50). High-resolution mass spectrometry-liquid chromatography data were obtained on an Agilent 6540 LC-MS QTOF coupled to an Agilent Jet-stream electrospray ionization detector. H_2O (A) and 0.1% FA in CH_3CN (B) were used as mobile phases on a Phenomenex Kinetex C18 column (2.6 μm, 100 Å, 150 x 3 mm:

 doi:10.20944/preprints202411.0376.v1

0.5 mL/min). Reverse-phase HPLC was performed on a Shimadzu LC20-AT system equipped with a photodiode array detector (M20A) using a preparatory Phenomenex C18 column (5 µm, 100 Å, 250 x 21.2mm: 10 mL/min) or a semi-preparatory Phenomenex C18 column (10 µm, 100 Å, 250 x 10 mm: 4 mL/min. The methanol and acetonitrile used for column chromatography were obtained from Fisher Co. and were HPLC grade (>99% purity) while the H_2O was distilled and filtered. Solvents mixtures are reported as *% v/v.*

3.2. Biological Materials, Extraction, and Isolation

Sponge specimens were collected from Palmer Station, Antarctica in 2018. The frozen sponge (1.7 g) was freeze-dried before extracted in MeOH twice overnight. An HP20 column was prepared by washing with $(CH_3)_2CO$ and pre-equilibrated in H_2O. The extract was passed through the column before the eluent was diluted with equal volume of H_2O and passed back through the column. The eluent was diluted a second time and passed through the column again. The column was eluted with 750 mL of 1) 30% Me_2CO/H_2O, 2) 75% Me_2CO/H_2O and 3) 100% Me_2CO. A ^1H NMR-guided fractionation was completed on the second fraction until pure compounds were achieved. Initial fractionation was performed using a preparative C18 HPLC with a 70-100% ACN/H_2O gradient over 15 minutes, resulting in 12 fractions. ^1H NMR was performed on each fraction, prioritizing fractions with a methyl around 2 ppm and an oxygen-bearing methine around 4.5 ppm. Semipreparative C18 HPLC was performed on fraction 8 using a gradient of 50-100% MeOH/H_2O, resulting in norsuberitenone B (**5**: 4.9 mg). The same method was used to purify **1**, **3**, and **6** affording to suberitenone K (**1**: 2.0 mg), furanosuberitandiol (**4**: 0.9 mg), abeosuberitandiol (**3**: 1.2 mg), respectively. Fraction 11 was purified by semipreparative C18 HPLC using a gradient of 75-100% MeOH/H_2O, resulting in suberitandiol (**2**: 3.2 mg) and the known compound suberitenone C (**8**). Fraction 10 was purified using the same method as described for fraction 11, resulting in the known compounds suberitenone D (**9**) and oxaspirosuberitenone (**10**). Fraction 9 and 12 contained the known compounds suberitenone B (**7**) and A (**6**), respectively.

3.3. Spectroscopic Data for the Suberites (1-5)

Suberitenone K (**1**): white film; $[\alpha]_D^{22}$ -31.1 (*c* 0.14, MeOH); UV (ACN/H_2O) λ_{max} 229 nm; ^1H NMR (600 MHz) and ^{13}C NMR (150 MHz), Table S1; HRESIMS *m/z* 465.2616 $[M + Na]^+$ (calcd for $C_{27}H_{38}O_5Na$, 465.2622; Δ 1.38 ppm).

Suberitandiol (**2**): white film; $[\alpha]_D^{22}$ -3.4 (*c* 0.32, MeOH); UV (ACN/H_2O) λ_{max} 274 nm; ^1H NMR (400 MHz) and ^{13}C NMR (100 MHz), Table S2; HRESIMS *m/z* 473.2908 $[M + CHOO]^-$ (calcd for $C_{28}H_{41}O_6$, 473.2908; Δ 0.13 ppm).

Abeosuberitandiol (**3**): white film; $[\alpha]_D^{22}$ +8.0 (*c* 0.09, MeOH); UV (ACN/H_2O) λ_{max} 261, 310 (sh) nm; ^1H NMR (400 MHz) and ^{13}C NMR (100 MHz), Table S3; HRESIMS *m/z* 487.2697 $[M + CHOO]^-$ (calcd for $C_{28}H_{38}O_7$, 487.2701; Δ 0.88 ppm).

Furanosuberitandiol (**4**): white film; $[\alpha]_D^{22}$ -8.6 (*c* 0.09, MeOH); UV (ACN/H_2O) λ_{max} 261 nm; ^1H NMR (400 MHz) and ^{13}C NMR (100 MHz), Table S4; HRESIMS *m/z* 501.2489 $[M + CHOO]^-$ (calcd for $C_{28}H_{37}O_8$, 501.2494; Δ 0.98 ppm).

Norsuberitenone B (**5**): white film; $[\alpha]_D^{22}$ +3.0 (*c* 0.24, MeOH); UV (ACN/H_2O) λ_{max} 225 nm; ^1H NMR (400 MHz) and ^{13}C NMR (100 MHz), Table S5; HRESIMS *m/z* 321.2433 $[M + H]^+$ (calcd for $C_{20}H_{33}O_3$, 321.2435; Δ 0.68 ppm).

3.4. RSV Antiviral Assay

The procedure was performed as previously described [7].

3.5. X-ray Diffraction

X-ray diffraction data on norsuberitenone B (**5**) was measured on Bruker D8 Venture PHOTON II CMOS diffractometer equipped with a Cu Kα INCOATEC ImuS micro-focus source (λ = 1.54178 Å). Indexing was performed using APEX4 (Difference Vectors method) [11]. Data integration and

 doi:10.20944/preprints202411.0376.v1

reduction were performed using SaintPlus [12]. Absorption correction was performed by multi-scan method implemented in SADABS [13]. Space group was determined using XPREP implemented in APEX3 [14]. Structure was solved using SHELXT and refined using SHELXL-2019/1 (full-matrix least-squares on F2) through OLEX2 interface program [15,16]. The ellipsoid plot was made with Olex2 [16]. Hydrogen atoms of -OH group and H_2O molecules were freely refined.

4. Conclusions

Herein, we reported five unreported sesterterpenes during our ongoing investigation of the chemical diversity of Antarctica and the sponge *Suberites* sp.. Three of the metabolites displayed an isolated phenol ring (**2**-**4**) with abeosuberitandiol showing a ring contraction and furanosuberitandiol displayed a new dihydrofuran ring. The biological activity of the unreported metabolites were tested together with the known compounds suberitenone A-D and oxaspirosuberitenone. Suberitenone A, B, and D has displayed interesting activity against respiratory syncytial virus (RSV). This research highlights the importance of marine organisms and their potential in drug discovery and supports further investigation of the relatively unexplored polar habitats.

Supplementary Materials: ^{1}H, ^{13}C, COSY, HSQC, HMBC and NOESY NMR spectra, and HR-MS of **1**-**5** are available free of charge at Preprints.org.

Author Contributions: Conceptualization, B.J.B., C.D.A., J.B.M. and M.N.T.; resources, B.J.B, C.D.A., J.B.M. and M.N.T.; formal analysis, S.S.H.O., M.N.T., K.C.T. and B.J.B.; methodology, S.S.H.O, M.N.T., K.C.T. and B.J.B.; investigation, S.S.H.O., S.K.M, J.L.S., K.C.T. and B.J.B; data curation, S.S.H.O, K.C.T. and B.J.B.; writing—original draft preparation, S.S.H.O.; writing—review and editing, all authors; supervision, B.J.B. and M.N.T.; funding acquisition, B.J.B., C.D.A., J.B.M. and M.N.T.; project administration, B.J.B. All authors have read and agreed to the published version of the manuscript.

Funding: The research in Antarctica was funded by the National Science Foundation awards PLR-1341333 (CDA and JBM) and PLR-1341339 (BJB). ESKAPE pathogen screening was supported by NIH grant AI154922 and *Candida* screening by NIH grant AT010939.

Data Availability Statement: The NMR data for the following compounds has been deposited in the Natural Products Magnetic Resonance Database (NP-MRD; www.np-mrd.org) and can be found under entries NP0341897 (suberitenone K), NP0341898 (suberitandiol), NP0341899 (abeosuberitandiol), NP0341900 (furanosuberitandiol), NP0341901 (norsuberitenone B). X-ray metadata was deposited at the Cambridge Crystallographic Data Centre, deposition number 2377382. Other data not found in the Supporting Information will be available upon request to the corresponding author.

Acknowledgments: The authors wish to thank the USF core facility staff, including the Directors of the Chemical Purification, Analysis, and Screening, the Interdisciplinary NMR Facility and the X-ray Diffraction and Solid State Characterization core facilities. The ASC support staff at Palmer Station, Antarctica, are acknowledged for the outstanding logistical services they provide to facilitate our field work. We would also like to thank Sarah Kennedy and Les Shaw for running the ESKAPE assay and Sarah Dietrick for her contributions to the *Candida* assay. JBM wishes to acknowledge support from an endowed Professorship in Polar and Marine Biology from the University of Alabama at Birmingham.

Conflicts of Interest: The authors declare no conflicts of interest.

References

1. Amsler, C.D.; Moeller, C.B.; McClintock, J.B.; Iken, K.B.; Baker, B.J. Chemical defenses against diatom fouling in Antarctic marine sponges. *Biofouling* **2000**, *16*, 29-45, doi:10.1080/08927010009378428.
2. McClintock, J.B.; Amsler, C.D.; Baker, B.J.; Van Soest, R.W. Ecology of Antarctic marine sponges: an overview. *Integr. Comp. Biol.* **2005**, *45*, 359-368, doi:10.1093/icb/45.2.359.
3. Jiménez, C. Marine natural products in medicinal chemistry. *Med. Chem. Lett.* **2018**, *9*, 959-961, doi:10.1021/acsmedchemlett.8b00368.
4. Blunt, J.W.; Carroll, A.R.; Copp, B.R.; Davis, R.A.; Keyzers, R.A.; Prinsep, M.R. Marine natural products. *Nat. Prod. Rep.* **2018**, *35*, 8-53, doi:10.1039/C7NO00052A.
5. Wilson, K.; de Rond, T.; Burkhardt, I.; Steele, T.S.; Schäfer, R.J.; Podell, S.; Allen, E.E.; Moore, B.S. Terpene biosynthesis in marine sponge animals. *Proc. Natl. Acad. Sci.* **2023**, *120*, e2220934120, doi:10.1073/pnas.2220934120.

 doi:10.20944/preprints202411.0376.v1

6. Núñez-Pons, L.; Shilling, A.; Verde, C.; Baker, B.J.; Giordano, D. Marine terpenoids from polar latitudes and their potential applications in biotechnology. *Mar. Drugs* **2020**, *18*, 401, doi:10.3390/md18080401.
7. Bracegirdle, J.; Olsen, S.S.; Teng, M.N.; Tran, K.C.; Amsler, C.D.; McClintock, J.B.; Baker, B.J. Neosuberitenone, a New Sesterterpenoid Carbon Skeleton; New Suberitenones; and Bioactivity against Respiratory Syncytial Virus, from the Antarctic Sponge Suberites sp. *Mar. Drugs* **2023**, *21*, 107, doi:10.3390/md21020107.
8. Lee, H.-S.; Ahn, J.-W.; Lee, Y.-H.; Rho, J.-R.; Shin, J. New sesterterpenes from the antarctic sponge Suberites sp. *J. Nat. Prod.* **2004**, *67*, 672-674, doi:10.1021/np030342t.
9. Shin, J.; Seo, Y.; Rho, J.-R.; Baek, E.; Kwon, B.-M.; Jeong, T.-S.; Bok, S.-H. Suberitenones A and B: Sesterterpenoids of an unprecedented skeletal class from the Antarctic sponge Suberites sp. *J. Org. Chem.* **1995**, *60*, 7582-7588, doi:10.1021/jo00128a034.
10. Díaz-Marrero, A.R.; Brito, I.; Cueto, M.; San-Martín, A.; Darias, J. Suberitane network, a taxonomical marker for Antarctic sponges of the genus Suberites? Novel sesterterpenes from Suberites caminatus. *Tetrahedron Lett.* **2004**, *45*, 4707-4710, doi:10.1016/j.tetlet.2004.04.091.
11. Bruker *APEX4*, 2015.9; Bruker AXS Inc: Madison, WI USA, 2022.
12. Bruker *SAINT*, 8.35A; Bruker AXS Inc.: Madison, WI USA, 2016.
13. Krause, L.; Herbst-Irmer, R.; Sheldrick, G.M.; Stalke, D. Comparison of silver and molybdenum microfocus X-ray sources for single-crystal structure determination. *J. Appl. Crystallogr.* **2015**, *48*, 3-10, doi:10.1107/s1600576714022985.
14. Sheldrick, G. SHELXT - Integrated space-group and crystal-structure determination. *Acta Crystallogr. Sec. A* **2015**, *71*, 3-8, doi:10.1107/S2053273314026370.
15. Sheldrick, G., M. Crystal structure refinement with SHELXL. *Acta Crystallographica Section C* **2015**, *71*, 3-8, doi:10.1107/S2053229614024218.
16. Dolomanov, O.V.; Bourhis, L.J.; Gildea, R.J.; Howard, J.A.K.; Puschmann, H. OLEX2: A complete structure solution, refinement and analysis program. *J. Appl. Crystallogr.* **2009**, *42*, 339-341. doi: 10.1107/s0021889808042726.